



COMPARATIVE SIMULATION OF A NON-LINEAR RADIATIVE ON TRI-HYBRID HYDROMAGNETIC NANOFLUID FLOW THROUGH A ROTATING DISK

K. Bhagya Swetha Latha*, *Department of Mathematics, Acharya Nagarjuna University Campus,
Ongole - 523 001, A.P., India*

M. Gnaneswara Reddy, *Department of Mathematics, Acharya Nagarjuna University Campus,
Ongole - 523 001, A.P., India*

*E-mail id: kswethalatha@gmail.com, mgrmaths@gmail.com

Abstract

In the present paper, the main focus on an advance enhancement of heat transport of the fluid, the concept of ternary hybrid nanofluid (tri-hybrid) model has been considered. The physical features of non-linear radiation on ternary hybrid nanoparticles are dissolved in Ethylene Glycol-Water (40: 60 %) base fluid flow through a rotating disk has been scrutinized. Cattaneo-Christov effect is introduced in energy equation to analyze the aspects of energy relaxation time in this study. The governing flow equations are constituted and are transform to an ODE's by utilizing Von Karman's transformations. The simplified flow and energy equations are resolved through aid of Runge-Kutta numerical scheme with shooting approach. The physical aspects and behaviour analysis for the radial and azimuthal velocities and temperature field of distinct flow variables of the modelled problem have been addressed by making use of two-dimensional (2-D) plots. Both velocities of the fluid are declines for the applied magnetic field. The energy transfer is improved near the disk for the temperature ratio and radiation of all three distinct nanofluids while the reverse impact is distinguished for the thermal relaxation time variable. It is important note that the ternary hybrid $CoFeO_2-Ag-TiO_2$ has better thermal conductivity of the fluid in comparison with unitary (mono) and Hybrid nanofluids from graphical results. The results of numerical simulation are validated against the published literature data and hence a nice agreement is perceived. The obtained results of the current model can be utilized in an advanced cooling system of hybrid electronic and nuclear engineering process.

Keywords: MHD, Non-linear radiation, Cattaneo-Christov heat flux, tri-hybrid nanofluid.

1. Introduction

The fluid transport through a rotating disk has considerable applications which include hybrid lubrication process, nuclear engineering, rotating hybrid machinery, turbo and advanced cooling reactor systems. Karman [1] have initially reported the fluid transport along an infinite disk in the year 1921. Later, the viscous steady flow features in a rotating disk have been examined by Cochran [2] in 1934 with the aid of the Von Karman transformations. Stuart [3] has presented the impact of suction on steady rotating disk flow configuration. The boundary layer and flow characteristics for a rotating disk along with applications has been studied by Gregory et al. [4]. Energy transfer and hydromagnetic flow of same geometry has been scrutinized by Sparrow and Cess [5]. The flow behavioural characteristics by considering the applied magnetic field has been explored by Kakutani [6]. Benton [7] have addressed the exact solutions of velocity function on the flow in a rotating disk. MHD feature is considered in a disk and graphical analysis has been examined by Pao [8]. The axial flow transport is declines for the magnetic field. Balachandar and Steett [9] have analyzed the laminar boundary layer flow through a rotating disk. They employing the spectral collocation scheme for the numerical simulation results. A series solution of flow in a porous disk has been reported by Kelson and Desseaux [10]. Jasmine and Gajjar [11] have described the flow convective boundary along a disk. Turkyilmazoglu [12] have explored the impact of hydromagnetic flow along a disk and conclude that resonance mechanism transport has stabilizing by magnetic field. By the same author [13] has been extended this work to a 3D viscous and boundary flow of rotating disk by revoking applied magnetic



field. Flow feature in the account of porous medium of the same geometry has been scrutinized numerically by Attia [14]. An analytical solution of heat transfer of a rotating disk has been discussed by Turkyilmazoglu [15,16]. Rashidi et al. [17] have reported the steady flow and thermal transport across a porous rotating disk.

The concept nanofluid is originated and pioneered work has been investigated by Choi [18] in the year 1995. The prominent works of nanofluids and its applications have reported in [19-22]. A two-dimensional (2D) boundary layer analysis of a nanofluid has been discussed by Khan and Pop [23]. The energy and boundary flow of a nanofluid through a disk has been explored by Bachok et al. [24]. The rate of heat transfer is diminished for boosting nanoparticle volume fraction. The interaction of nanofluid flow in a disk in the presence of heat flux has been investigated by Andrews and Devi [25]. Hydromagnetic steady transport analysis in a porous disk by considering nanoparticles has been explored by Rashidi et al. [26]. The energy movement of Cu , Al_2O_3 and CuO nanoparticles H_2O based nanofluid has been studied by Yin et al. [27]. The flow governing equations are simplified by Von Karman transformations and final equations are resolved through homotopy method. The flow behaviour and radiative flow of a rotating disk in the presence of dissipation has been explored by Khan and his co-authors [28, 29]. It is perceived that fluid temperature is boosting by varying thermal radiation. The flow and non-linear radiation impact on a porous nanofluid disk has been studied numerically by Upadhyaya et al. [30]. The numerical analysis on non-linear radiative transport due to a disk has been assessed by Alsallami et al. [31].

The thermal enhancement for the mono nanofluid (unitary nanofluid) is low as compared to that of binary composite nano-fluid (Hybrid nanofluid). The hybrid nano-fluids have considerable research due to the efficiency high in heat transfer mechanism. Asifa et al. [32] have reported the thermal flow in a rotating hybrid nanofluid $CNT + Fe_3O_4/H_2O$ disk. It has been perceived that the hybrid nanofluid of the heat transfer enhancement is high as contrast to that of common fluid. A mathematical analysis of hybrid hydromagnetic nanofluid along a spinning disk by considering dissipation has been described by Shoaib et al. [33]. Waqas et al. [34] have reported the radiative and hydromagnetic hybrid nanofluid flow through a rotating disk. The radial fluid velocity is diminishing for the applied magnetic field. Ijaz Khan [35] have scrutinized the heat transfer enhancement on Darcy-Forchheimer flow in a rotating disk through hybrid nanoparticles. Aluminium oxide (Al_2O_3) + Copper(Cu) nanoparticles have been utilized for the preparation of a hybrid nanofluid. Both tangential and radial reduced for escalating the Darcy-Forchheimer variable along with associated boundary layers. The hybrid $Cu - Al_2O_3$ nanofluid with regular water-based fluid is used in this study. They noticed that the temperature field enhances for Eckert number. Mahesh Kumar and Pranab Kumar [36] have addressed the computational study on the hybrid nanofluid movement. The hybrid Zinc Oxide- Ag nanofluid flow towards a rotating disk has been recently examined experimentally by Mousavi et al. [37].

As mentioned of the preceding two paragraphs of literature over the disk geometry, the researchers have been done on fluid flow and thermal transport of unitary and hybrid nanofluids. The three distinct nanoparticles are formed by disseminated into base fluid are called the ternary hybrid nanofluids. Ternary hybrid nanofluids are the new advanced class of nanofluids. The thermal features for tri-hybrid CuO , Al_2O_3 and Cu nanofluid with H_2O in a spinning disk has recently examined by Shahzad et al. [38]. Alshahrani et al. [39] have scrutinized a steady flow of tri- hybrid carbon nanofluids (CNTS), Zirconium(ZrO_2) and aluminum oxide (Al_2O_3) through a spinning disc. They conclude that the temperature field boosts for the addition of ternary hybrid nanoparticles. Heat transfer analysis and flow on a ternary nanofluid along a rotating disk through the linear radiation mechanism has been analyzed very recently by Shamshuddin et al. [40].

The main objective of the present exploration is to perceive the fluid flow and thermal characteristics of ternary hybrid nanofluid, hybrid fluid and unitary nanofluid in a base fluid $C_2H_6O_2-H_2O$ over a

rotating spinning disk by considering Cattaneo-Christov heat flux and non-linear radiation. The governing equations are constructed from the Navier-Stokes equations and these are simplified to non-linear system of ODE's by utilizing Karman transformations. The Runge-Kutta fourth order numerical scheme has been utilized for resultant equations and simulate the graphical analysis for the three nanofluids for the influences of physical flow parameters. Also, the two friction factors and thermal transfer rate have exhibited tabularly and analyzed for the controlling variables of the present model. The comparison graphical and tabular results show that ternary hybrid nanoparticles are more helpful in growing the flow and thermal characteristic factors i.e., fluid velocity and temperature of the fluid as contrast to the unitary and binary composite nanoparticles. Furthermore, the thermal efficiency for the tri-hybrid nanofluid is more than the normal hybrid nanofluids.

2. Modeling

A steady and viscous flow of tri-hybrid ($CoFeO_4-Ag-TiO_2$) nanofluid through a rotating disk with Ω as the angular velocity at z -axis is scrutinized. Here the mixture of 40 % Ethylene ($C_2H_6O_2$) and 60% water (H_2O) is employed as a base fluid. It is considered that the velocity components (u, v, w) in the directions of cylindrical coordinates system (r, φ, z). In the energy equation, the non-linear radiation impact has been considered. The applied magnetic field strength B_0 is applied on the opposite the fluid flow direction. Fig.1 is exhibited for the physical model and geometrical flow configuration. In view of the above suppositions, the governing flow equations of are given by [17, 24, 26, 34]

$$\frac{\partial u}{\partial r} + \frac{\partial w}{\partial z} + \frac{u}{r} = 0 \tag{1}$$

$$u \frac{\partial u}{\partial r} + w \frac{\partial u}{\partial z} - \frac{v^2}{r} = -\frac{1}{\rho_{thnf}} \frac{\partial P}{\partial r} \vartheta_{thnf} \left(\frac{\partial^2 u}{\partial r^2} + \frac{1}{r} \frac{\partial u}{\partial r} - \frac{u}{r^2} + \frac{\partial^2 u}{\partial z^2} \right) - \frac{\sigma_{thnf}}{\rho_{thnf}} B_0^2 u \tag{2}$$

$$u \frac{\partial v}{\partial r} + w \frac{\partial v}{\partial z} + \frac{uv}{r} = \vartheta_{thnf} \left(\frac{\partial^2 v}{\partial r^2} + \frac{1}{r} \frac{\partial v}{\partial r} - \frac{v}{r^2} + \frac{\partial^2 v}{\partial z^2} \right) - \frac{\sigma_{thnf}}{\rho_{thnf}} B_0^2 v \tag{3}$$

$$u \frac{\partial w}{\partial r} + w \frac{\partial w}{\partial z} = -\frac{1}{\rho_{thnf}} \frac{\partial P}{\partial z} \vartheta_{thnf} \left(\frac{\partial^2 w}{\partial r^2} + \frac{1}{r} \frac{\partial w}{\partial r} + \frac{\partial^2 w}{\partial z^2} \right) \tag{4}$$

$$\begin{aligned} & (\rho c_p)_{thnf} \left(u \frac{\partial T}{\partial r} + w \frac{\partial T}{\partial z} \right) \\ & = k_{thnf} \left(\frac{\partial^2 T}{\partial r^2} + \frac{1}{r} \frac{\partial T}{\partial r} + \frac{\partial^2 T}{\partial z^2} \right) - \frac{\partial q_r}{\partial z} \\ & + \varepsilon_t \left[u^2 \frac{\partial^2 T}{\partial r^2} + 2vw \frac{\partial^2 T}{\partial r \partial z} + w^2 \frac{\partial^2 T}{\partial z^2} + u \frac{\partial w}{\partial r} \frac{\partial T}{\partial z} + u \frac{\partial u}{\partial r} \frac{\partial T}{\partial r} \right. \\ & \left. + w \frac{\partial u}{\partial z} \frac{\partial T}{\partial z} + w \frac{\partial w}{\partial z} \frac{\partial T}{\partial z} \right] \end{aligned} \tag{5}$$

and the relevant boundary restrictions [17,35] are given by

$$\begin{aligned} u = 0, \quad v = \Omega r, \quad w = 0, \quad T = T_w \quad \text{at } z = 0 \\ u \rightarrow 0, \quad v \rightarrow 0, \quad T \rightarrow T_\infty \quad \text{as } z \rightarrow \infty \end{aligned} \tag{6}$$

in which $\vartheta_{thnf} = \frac{\mu_{thnf}}{\rho_{thnf}}$, ρ_{thnf} , $(\rho c_p)_{thnf}$, σ_{thnf} , k_{thnf} , T are represents, kinematic viscosity, heat capacitance, the density electrical conductivity, thermal conductivity of tri-hybrid nanofluid, the fluid temperature, ε_t is the thermal relaxation time, q_r is the radiative heat flux.

The radiative heat flux q_r for the thermal radiation [34,35] is given by

$$q_r = -\frac{4\sigma^*}{3k^*} \frac{\partial T^4}{\partial z} = -\frac{16T_\infty^3}{3k^*} \frac{\partial T}{\partial z} \tag{7}$$

Here k^* is the mean absorption coefficient and σ^* denotes the Stefan-Boltzmann constant.

The thermo-physical properties of nanoparticles Silver (*Ag*), Cobalt ferrite (*CoFeO₄*), Titanium dioxide (*TiO₂*), Ethylene-Water 40:60% base fluid is exhibited in Table 1.

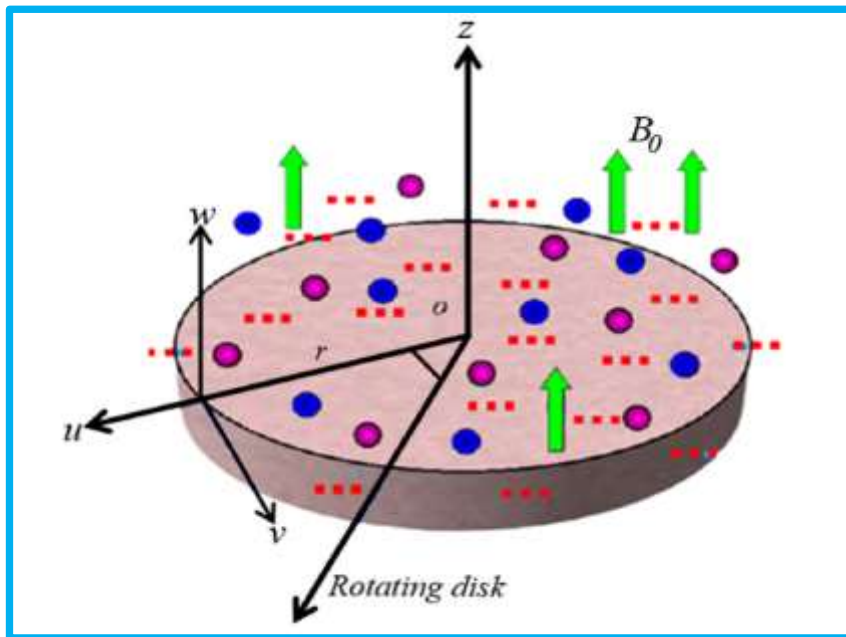


Fig.1. Physical flow configuration.

Table-1: Thermo-physical characteristics of three distinct nanoparticles and base fluid [44].

| Physical characteristics | Ethylene Glycol EGW (40:60%) | <i>Ag</i> | <i>CoFeO₄</i> | <i>TiO₂</i> |
|--------------------------|------------------------------|-------------------|--------------------------|------------------------|
| ρ | 1041.89 | 10.5 | 4907 | 4250 |
| σ | 5.5×10^{-6} | 3.6×10^7 | 5.51×10^9 | 2.38×10^6 |
| c_p | 3421.54 | 235 | 700 | 686.2 |
| k | 0.1816 | 429 | 3.7 | 8.9538 |

The mathematical relations for the thermophysical properties for nanofluid, hybrid nano fluid and ternary hybrid (tri-hybrid) nanofluid as follows [40,42,44]

Define the following similarity transformations and non-dimensional variables in the governing modelled equations [24, 35]

$$u = r\Omega \frac{df}{d\zeta}, v = r\Omega g(\zeta), w = -2\sqrt{\Omega\vartheta_f} f(\zeta), \zeta = \sqrt{\frac{2\Omega}{\vartheta_f}} z, P = P_\infty + 2\Omega\mu_f f(\zeta)$$



$$M = \frac{\sigma_f B_0^2}{\rho_f \Omega}, \theta(\zeta) = \frac{T - T_\infty}{T_w - T_\infty}, Pr = \frac{\nu_f}{\alpha_f}, Rd = \frac{16\sigma^* T_\infty^3}{3k^* k_f}, \Gamma_t = \varepsilon_t \Omega, \quad (8)$$

$$T = T_\infty(1 + (\theta_w - 1)\theta), \theta_w = \frac{T_w}{T_\infty}$$

By making using equations (8) and (7), it is evident that the equation (1) is satisfied and equations (2) - (6) are reduced to

$$\frac{N_1}{N_2} f'''' + 2ff'' + g^2 - \frac{N_3}{N_2} Mf' = 0 \quad (9)$$

$$\frac{N_1}{N_2} g'' + 2fg' + g^2 - 2f'g - \frac{N_3}{N_2} Mg = 0 \quad (10)$$

$$\theta'' + RdN_4 \frac{d}{d\zeta} ([1 + \theta(\zeta)(\theta_w - 1)]^3 \theta'(\zeta)) + 2N_4 N_5 Pr f \theta' - Pr \Gamma_t (f^2 \theta'' + f f' \theta') = 0 \quad (11)$$

and dimensionless boundary conditions are

$$f = 0, f' = 0, g = 1, \theta = 1 \quad \text{at } \zeta = 0 \quad (12)$$

$$f' \rightarrow 0, g \rightarrow 0, \theta \rightarrow 0 \quad \text{as } \zeta \rightarrow \infty$$

Where M is the magnetic variable, Pr is the Prandtl number, Rd is the thermal radiation parameter, θ_w is the temperature ratio parameter, Γ_t is the thermal relaxation time variable, N_1, N_2, N_3, N_4 and N_5 are constants and are given by

$$N_1 = \frac{\mu_{thnf}}{\mu_f}, N_2 = \frac{\rho_{thnf}}{\rho_f}, N_3 = \frac{\sigma_{thnf}}{\sigma_f}, N_4 = \frac{k_f}{k_{thnf}}, N_5 = \frac{(\rho c_p)_{thnf}}{(\rho c_p)_f} \quad (13)$$

The dimensionless surface drag force on the radial and azimuthal directions, and the rate of thermal transport are defined as

$$Re_r^{1/2} C_{f_r} = N_1 f''(0) \quad (14)$$

$$Re_r^{1/2} C_{g_r} = N_1 f'(0) \quad (15)$$

$$Re_r^{-1/2} Nu = -\frac{1}{N_4} (1 + Rd) [1 + \theta(0)(\theta_w - 1)]^3 \theta'(0) \quad (16)$$

Here $Re_r = \frac{\Omega r^2}{\nu_f}$ is represents local Reynolds number.

3. Solution of the Problem

The dimensionless final governing flow equations (9) - (11) are highly coupled and non-linear. Hence, it is not possible find the exact solutions. Therefore, these coupled systems of ODE's have solved numerically by utilizing Rung-Kutta fourth order (R-K-F) numerical procedure.

To assess the utilized numerical scheme for the solving of the dimensionless governing equations, the comparison of $f'(0)$ for distinct values of M with the published literatures of Mustafa [41], Rashidi et al. [26], and Waini et al. [43] as shown in Table 2. It is perceived that a nice agreement is for the mentioned published research literatures and present results.

4. Graphical Analysis

The physical characteristics of pertinent flow variables on the radial velocity function $f'(\zeta)$, azimuthal velocity function $g(\zeta)$ and temperature function $\theta(\zeta)$ for three different nanofluids such as ternary hybrid nanofluid Hybrid nanofluid, and mono nanofluid Cobalt ferrite have been discussed



through graphically from Figs. 2-8. Also, the impacts of drag force and thermal transport have displayed for three different models of the sundry flow parameters.

Table 2: Numerical values of $f'(0)$ for different values of M .

| M | Mustafa [41] | Rashidi et al. [26] | Waini et al. [43] | Present results |
|-----|--------------|---------------------|-------------------|-----------------|
| 0 | 0.510186 | 0.510233 | 0.510216 | 0.5102136 |
| 1 | 0.309242 | 0.309258 | 0.309258 | 0.3092564 |
| 4 | 0.162701 | 0.162703 | 0.162703 | 0.1627012 |
| 5 | 0.123541 | 0.123582 | 0.123564 | 0.1235414 |

The characteristics of M on the three flow distributions are elucidated in Fig.2. It is observed from Fig.2 that, the radial fluid velocity is reduced for higher applied magnetic field. The physical reason behind that, the higher magnetic field causes Lorentz forces and which declines the fluid velocity. The dimensionless radial fluid flow diminished near the rotating disk for magnetic variable M . Here from Fig.3, it is clearly noticed that magnetic field variable declines the azimuthal velocity function $g(\zeta)$. Further, the impact of mono nanofluid (Cobalt ferrite ($CoFeO_4/EGW$)) is high for azimuthal velocity function $g(\zeta)$. The non-dimensional thermal function $\theta(\zeta)$ is enhanced for larger M . Physically, the fluid temperature improves for higher magnetic Lorentz force. The same behaviour is observed from the literature [34]. The temperature is low for the mono nanofluid. Also, the behaviour of radial $f'(\zeta)$, azimuthal $g(\zeta)$ velocities have same for the magnetic variable while the reverse effect is noted for temperature $\theta(\zeta)$.

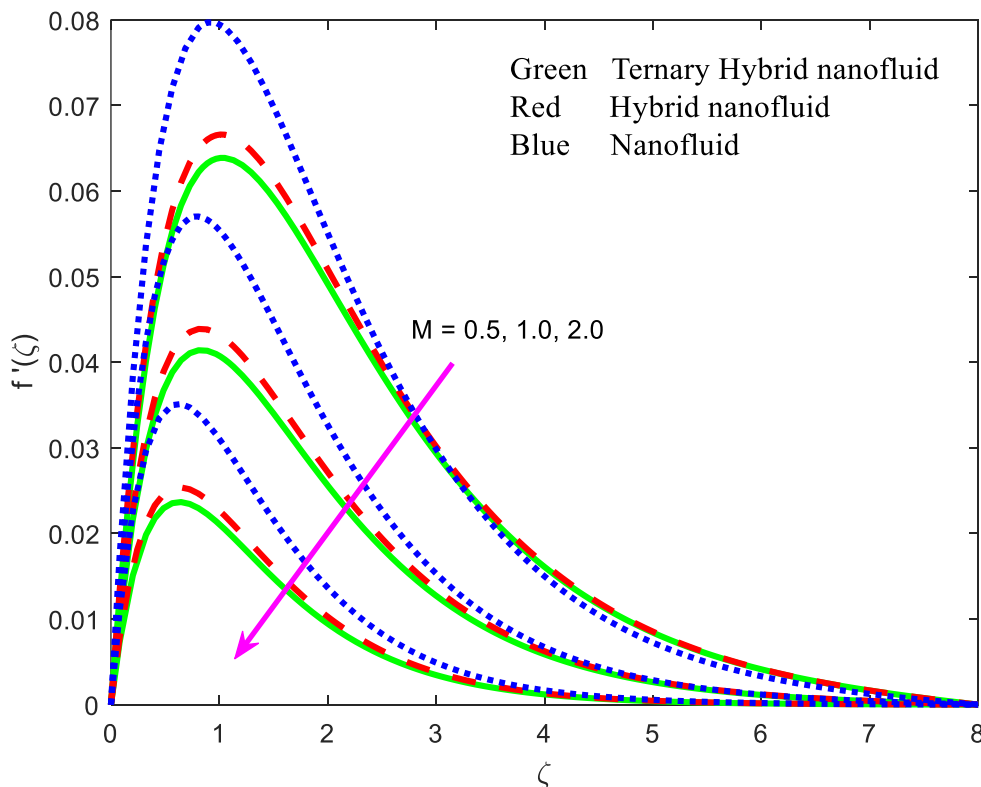


Fig.2. Variation of M on $f'(\zeta)$.

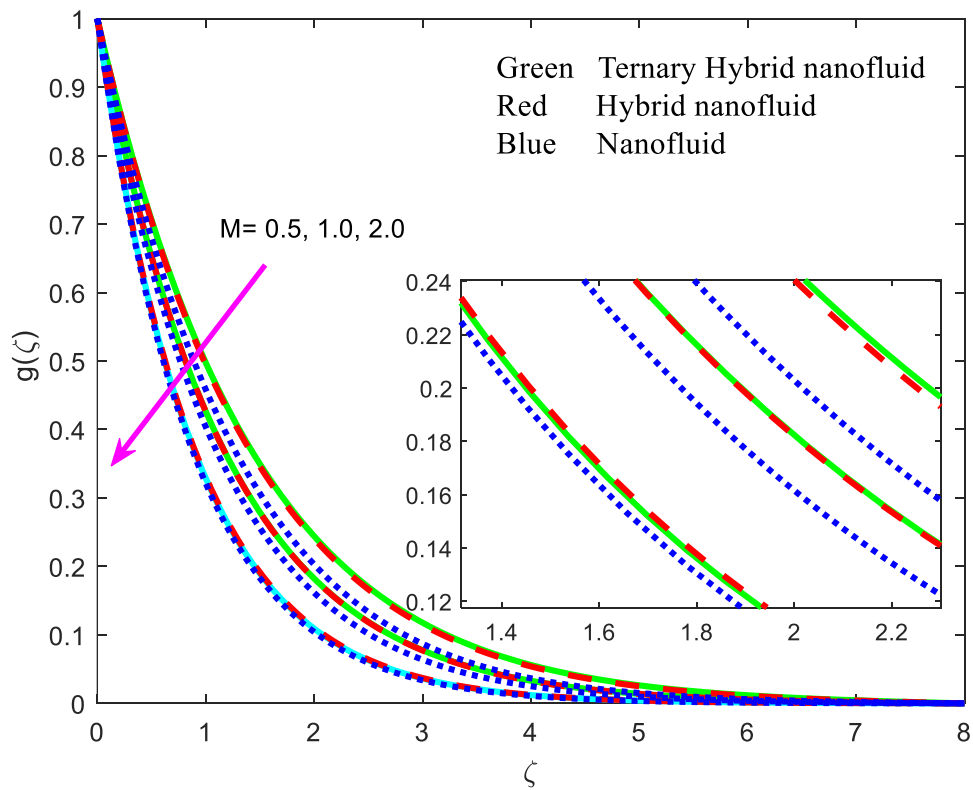


Fig.3. Variation of M on $g(\zeta)$.

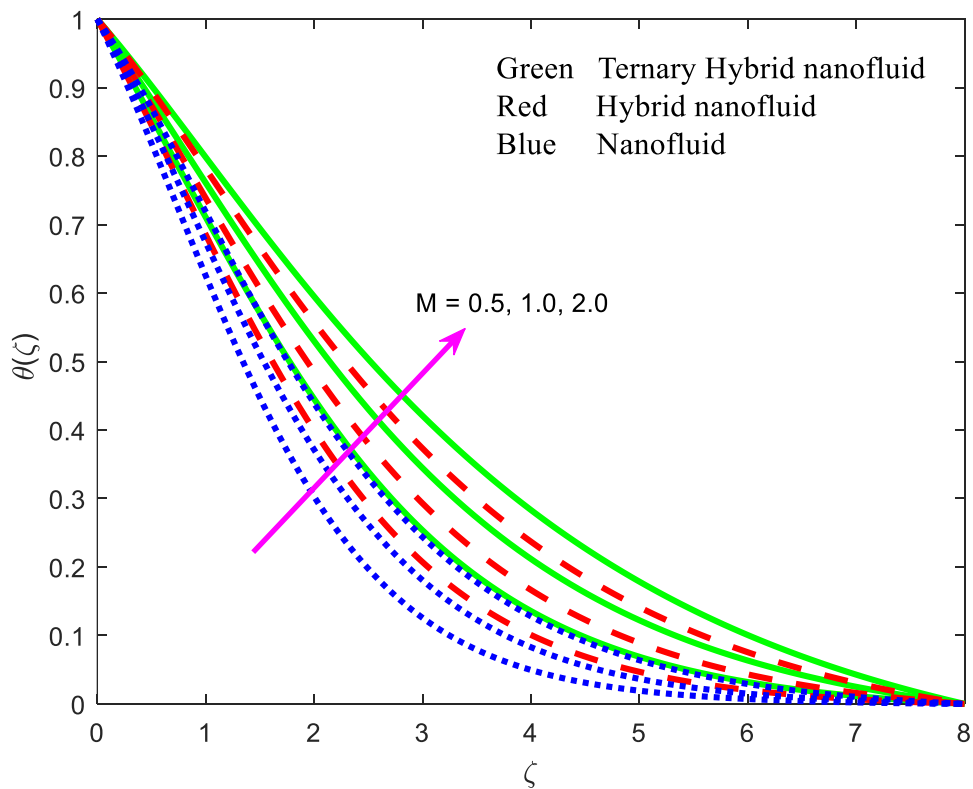


Fig.4. Variation of M on $\theta(\zeta)$.

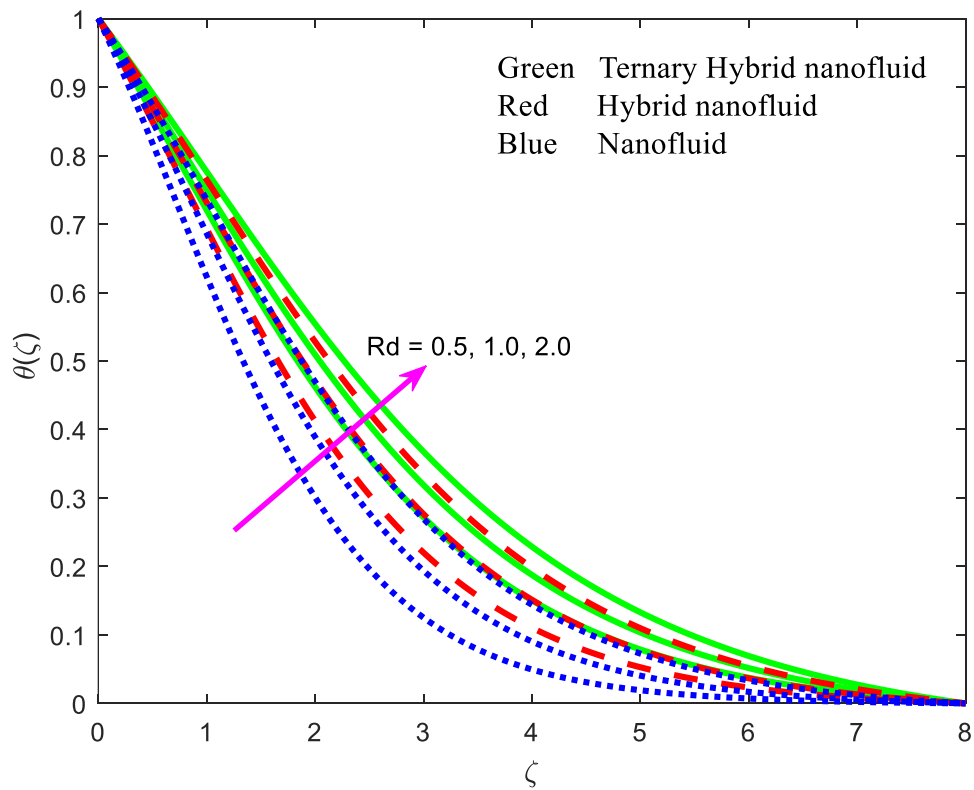


Fig.5. Variation of R_d on $\theta(\zeta)$.

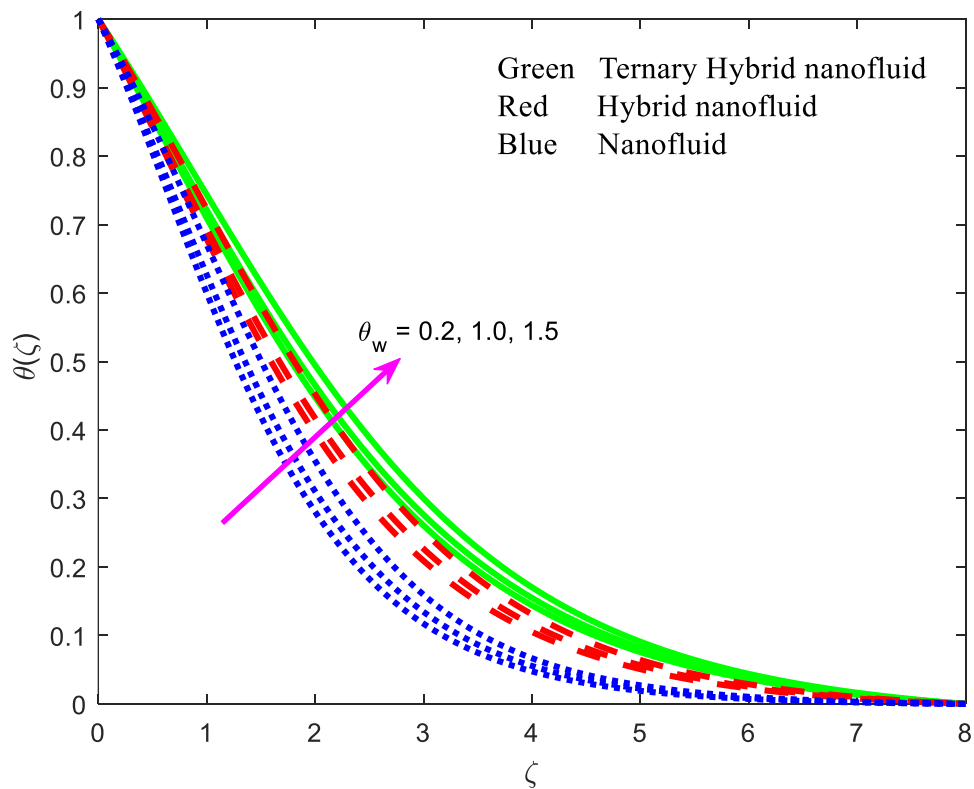


Fig.6. Variation of θ_w on $\theta(\zeta)$.

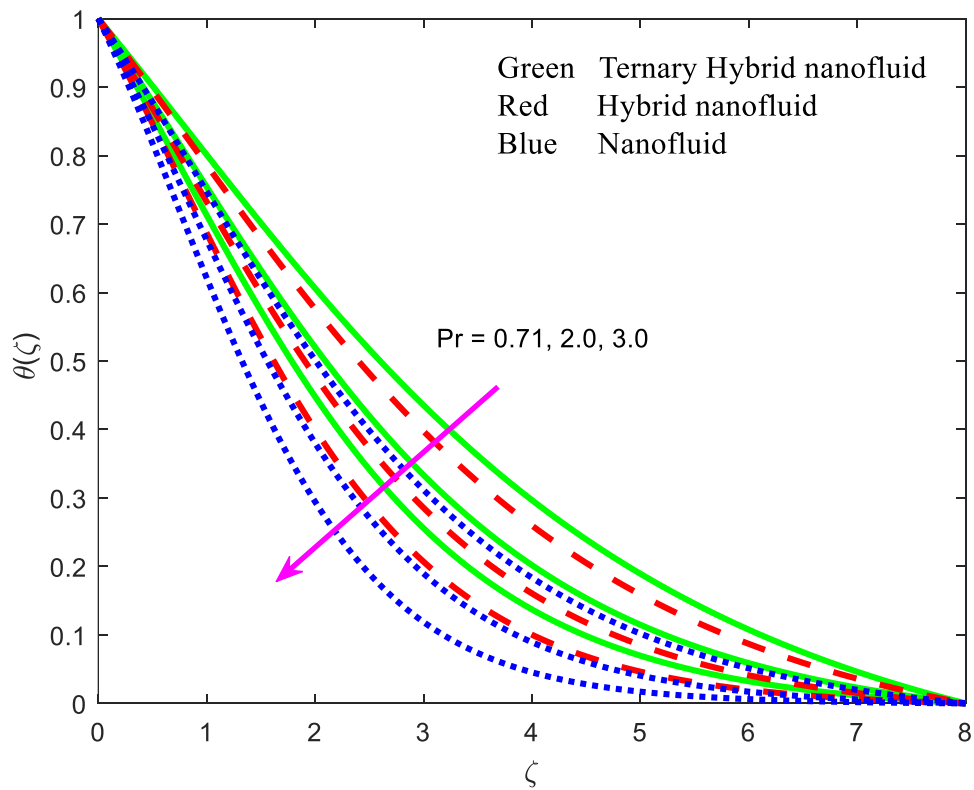


Fig.7. Variation of Pr on $\theta(\zeta)$.

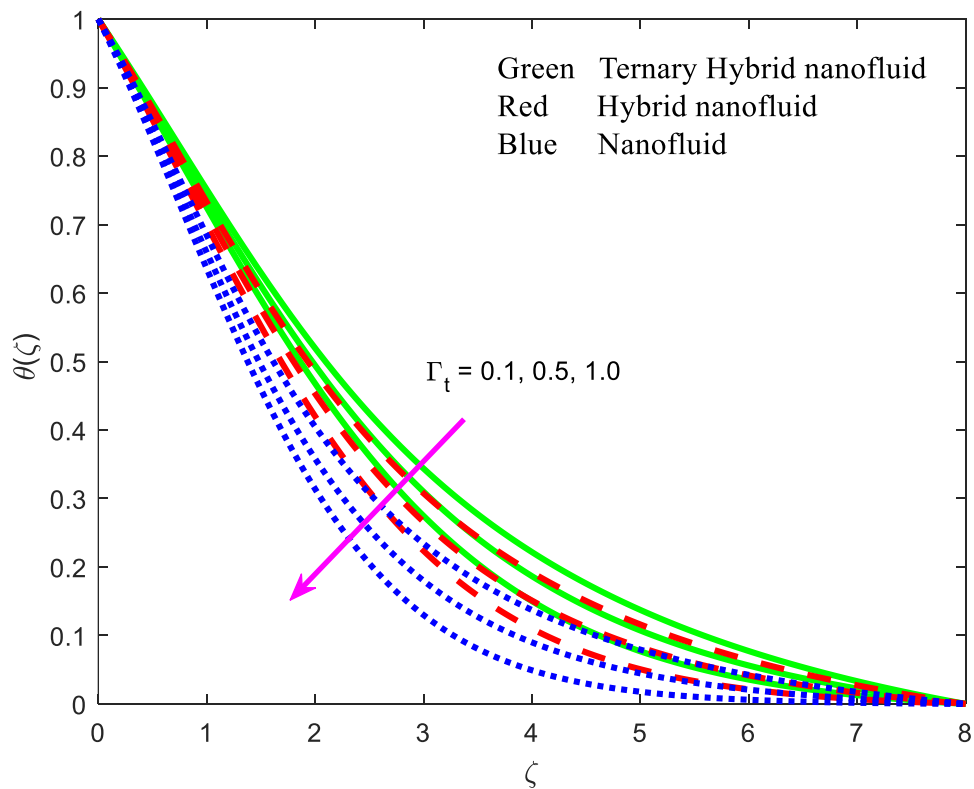


Fig.8. Variation of Γ_t on $\theta(\zeta)$.



Table 3: Computation values of radial skin-friction (Cf_r) for different values of M .

| M | Cf_r | | |
|-----|----------------------|------------------|-----------|
| | Tri-Hybrid Nanofluid | Hybrid Nanofluid | Nanofluid |
| 0.5 | 0.396421 | 0.320581 | 0.327250 |
| 1.0 | 0.303571 | 0.247058 | 0.260310 |
| 2.0 | 0.229428 | 0.187742 | 0.204032 |
| 3.0 | 0.191397 | 0.156917 | 0.172501 |

Table 4: Numerical results of azimuthal skin- friction (Cg_r) for different values of M .

| M | Cg_r | | |
|-----|----------------------|------------------|-----------|
| | Tri-Hybrid Nanofluid | Hybrid Nanofluid | Nanofluid |
| 0.5 | 1.396486 | 1.077151 | 0.893623 |
| 1.0 | 1.898599 | 1.459163 | 1.189228 |
| 2.0 | 2.483253 | 1.897846 | 1.499916 |
| 3.0 | 2.959847 | 2.257281 | 1.761874 |

Table 5: Numerical results of Nusselt number (Nu) for different values of Rd , θ_w , and Γ_t .

| Rd | θ_w | Γ_t | Nu | | | | |
|------|------------|------------|----------------------|------------------|-----------|----------|----------|
| | | | Tri-Hybrid Nanofluid | Hybrid Nanofluid | Nanofluid | | |
| 0.1 | 1.2 | 0.2 | 0.558213 | 0.471284 | 0.404657 | | |
| 0.5 | | | 0.792700 | 0.654384 | 0.535709 | | |
| 1.5 | | | 1.045858 | 0.849044 | 0.669613 | | |
| | | 0.5 | | 0.509073 | 0.433363 | 0.379198 | |
| | | | 1.5 | | 0.717474 | 0.593856 | 0.489219 |
| | | | | 2.0 | 0.934980 | 0.755426 | 0.595028 |
| | | | 0.4 | | 0.612452 | 0.510801 | 0.427272 |
| | | | | 0.6 | 0.604904 | 0.501917 | 0.414873 |
| | | | | 0.8 | 0.597949 | 0.493756 | 0.403369 |

Fig.5. displays the impact of thermal radiation parameter Rd on non-dimensional temperature $\theta(\zeta)$ for three different nanofluids. The numerical results of the plot shows that fluid temperature escalates as the values of Rd increase. The same temperature behaviour to that delineated by [34] and [36]. Also, the temperature of mono $CoFeO_4$ nanofluid with EG-W base fluid is small and it is highest for the tri-hybrid $CoFeO_4-Ag-TiO_2$ nanofluid. The behaviour of fluid temperature $\theta(\zeta)$ for the comparison of three nanofluids of the temperature ratio parameter θ_w been demonstrated in Fig.6. The intensification in the temperature of nanofluids as distinguished for boosting estimation of the temperature ratio variable θ_w . This is because of a large quantity of thermal conductivity to the nano-liquids in the existence of temperature ratio and which leads to enhancement of temperature. Further, overserving that the temperature for unitary nanofluid as lowest as contrasted to other hybrid nanofluids. Fig.7 highlight the influence of Prandtl number Pr on temperature distribution $\theta(\zeta)$. It is analyzed that the



growing estimation of reduced the temperature of three nanofluids (mono, Hybrid and tri-Hybrid nano fluids). This is agreeing as per the physical scenario concept with the published works of [28] and [32]. Fig.8 is plotted to disclose a discrimination in fluid temperature distribution for increasing values of thermal relaxation variable Γ_t . It is revealed that temperature is decreased for growing thermal relaxation variable Γ_t .

Finally, the behaviour of friction factor coefficients Cf_r , Cg_r and Nusselt number Nu for the impact of sundry flow physical variables along contrast of three nanofluids with Ethylene Glycol - Water (EG-W) base fluid has been exhibited in Tables 3-5 respectively. It is evident from Table 4, that the skin-friction coefficient Cf_r is reduced of three distinct types of nanofluids for intensification of magnetic variable M . it is further note that the hybrid $CoFeO_4-Ag$ nanofluid has lower values of Cf_r in comparison with ternary nanofluid. As exceeded values of magnetic variable M , azimuthal skin-friction Cg_r grow for all three nanofluids (see Table 4). It is also concluded that tri-hybrid $CoFeO_4-Ag-TiO_2$ nanoparticle is highest in comparison of other nanofluids. A comparative examination of nanofluids on the Nusselt number to the impact of Rd , θ_w , and Γ_t has been displayed in Table 5. The Nusselt number Nu is boosted for the energy radiation and temperature ratio while the converse effect for Γ_t . Furthermore, the ternary nanofluid impact on the rate of heat transfer is high as compared with other two nanofluids.

5. Conclusion

The physical characteristics of non-linear radiation on ternary ($CoFeO_2-Ag-TiO_2$) hybrid nanoparticles are dissolved in $C_2H_6O_2 - H_2O$ 40: 60% base fluid flow through a rotating disk has scrutinized. The Cattaneo-Christov model is accounted in energy equation to analyze the aspects of energy relaxation time. The governing equations are modelled and transform to a system of ODE's by utilizing Von Karman's transformations. The final equations are resolved numerically. The main observations of the present analysis are:

1. The radial fluid velocity $f'(\zeta)$ is reduced for higher magnetic field.
2. The radial fluid velocity $f'(\zeta)$ is higher for the unitary $CoFeO_4$ nanofluid as contrasted to other two hybrid nanofluids $CoFeO_4-Ag-TiO_2/EGW$ and $CoFeO_4-Ag/EGW$.
3. The temperature of mono $CoFeO_4$ nanofluid with EG-W base fluid of the thermal radiation Rd is small.
4. The temperature function $\theta(\zeta)$ is decreased for growing thermal relaxation variable Γ_t .
5. The Nusselt number Nu is boosted for the energy radiation and temperature ratio while the converse effect for Γ_t .

References

- [1] T. Von Kármán, Über laminar and turbulent Reibung, *ZAMM-Zeitschrift für Angewandte Mathematik und Mechanik* 1 (4) 233–252 (1921).
- [2] W.G. Cochran, The flow due to a rotating disc, in: *Mathematical Proceedings of the Cambridge Philosophical Society* 30, Cambridge University Press, 365–375 (1934).
- [3] J. T. Stuart, on the effects of uniform suction on the steady flow due to a rotating disk, *The Quarterly Journal of Mechanics and Applied Mathematics*, 7(4) 446–457 1954.
- [4] N. Gregory, J.T. Stuart, and W.S. Walker, On the stability of three-dimensional boundary layers with applications to the flow due to a rotating disk. *Philos Trans Roy Soc London Ser A*, 248 155–199 (1955).
- [5] E.M. Sparrow and R.D. Cess, Magnetohydrodynamic flow and heat transfer about a rotating disk. *J Appl Mech.*, 29 181–187 (1962).
- [6] T. Kakutani, Hydromagnetic flow due to a rotating disk, *Journal of Physics Society of Japan*, 17 1496–1506 (1962).



- [7] E. Beton, On the flow due to a rotating disk, *Journal of Fluid Mechanics*, 24(4) 781-800 (1966).
- [8] H.P. Pao, Magnetohydrodynamic flows over a rotating disk. *AIAA J* 6, 1285-1291 (1968).
- [9] S. Balachandar and C.L. Streett, Numerical Simulation of Transition in a Rotating Disk Flow. In: Hussaini, M.Y., Voigt, R.G. (eds) *Instability and Transition*. ICASE/ NASA LaRC Series. Springer, New York, NY (1990).
- [10] N. Kelson, and A. Desseaux, Note on porous rotating disk flow, *Aust. N. Z. Ind. Appl. Math. J.*, 42 837–855, (2000).
- [11] H.A. Jasmine and J.S.B. Gajjar, Absolut and convective instabilities in the incompressible boundary layer on a rotating disk with a temperature-dependent viscosity, *Int. J. Heat Mass Transf.*, 48 1022–1037 (2005).
- [12] M. Turkyilmazoglu, Resonance instabilities in the boundary-layer flow over a rotating-disk under the influence of a uniform magnetic field, *J Eng Math.*, 59 337–350 (2007). <https://doi.org/10.1007/s10665-007-9137-7>.
- [13] M. Turkyilmazoglu, Primary instability mechanisms on the magnetohydrodynamic boundary layer flow over a rotating disk subject to a uniform radial flow, *Physics of Fluids*, 21 074103, (2009).
- [14] H.A. Attia, Steady flow over a rotating disk in porous medium with heat transfer, *Nonlinear Analysis: Model. Control*, 14(1), 21–26 (2009).
- [15] M. Turkyilmazoglu, Purely analytic solutions of magnetohydrodynamic swirling boundary layer flow over a porous rotating disk, *Comput. Fluids*, 39 (5) 793–799 (2010).
- [16] M. Turkyilmazoglu, Exact flow/heat solutions for the non-axisymmetric flow over a rotating disk, *Acta Mech.*, 223 161–166 (2012).
- [17] M.M. Rashidi, S.A. Mohimani Pour, T. Hayat and S. Obaidat, Analytic approximate solutions for steady flow over a rotating disk in porous medium with heat transfer by homotopy analysis method, *Computers & Fluids*, 54 1-9 (2012).
- [18] S.U. Choi and J.A. Eastman, *Enhancing Thermal Conductivity of Fluids with Nanoparticles*, Argonne National Lab, IL (United States) (1995).
- [19] Q.Z. Xue, Model for thermal conductivity of carbon nanotube-based composites, *Phys. B Condens. Matter* 368 302–307 (2005).
- [20] X. Wang, X. Xu, and S.U.S. Choi, Thermal conductivity of nanoparticle-fluid mixture, *J. Thermophys. Heat Transf.*, 13 474–480 (1999).
- [21] V. Trisaksri and S.J.R. Wongwises, Critical review of heat transfer characteristics of nanofluids, *Renew. Sust. Energ. Rev.*, 11 (3) 512–523 (2007).
- [22] S. Murshed, K. Leong and C.J. Yang, Thermophysical and electrokinetic properties of nanofluids—a critical review, *Appl. Therm. Eng.*, 28 2109–2125 (2008).
- [23] W.A. Khan and I. Pop, Boundary layer flow of a nanofluid past a stretching sheet, *Int. J. Heat Mass Transf.*, 53 2477–2483 (2010).
- [24] N. Bachok, A. Ishak and I. Pop, Flow and heat transfer over a rotating porous disk in a nanofluid, *Physica B*, 406 (9) 1767–1772 (2011).
- [25] J. Andrews and S.A. Devi, Nanofluid Flow over a rotating disk with prescribed heat flux. *Mapana-J. Sci.*, 11(3), 77–92 (2012).
- [26] M.M. Rashidi, S. Abelman and N. Freidooni Mehr, Entropy generation in steady MHD flow due to a rotating porous disk in a nanofluid, *International Journal of Heat and Mass Transf.*, 62, 515-525 (2013).
- [27] C. Yin, L. Zheng, C. Zhang and X. Zhang, Flow and heat transfer of nanofluids over a rotating disk with uniform stretching rate in the radial direction, *Propulsion Power Res.*, 6(1), 25–30 (2017).
- [28] M. Khan, W. Ali and J. Ahmed, A hybrid approach to study the influence of Hall current in radiative nanofluid flow over a rotating disk, *Appl Nanosci.*, 10 5167–5177 (2020).



- [29] M. Khan, J. Ahmed, and W. Ali, Thermal analysis for radiative flow of magnetized Maxwell fluid over a vertically moving rotating disk, *J Therm Anal Calorim.*, 143, 4081–4094 (2021).
- [30] S.M. Upadhya, R.L.V.R. Devi, C.S.K. Raju, Magnetohydrodynamic nonlinear thermal convection nanofluid flow over a radiated porous rotating disk with internal heating, *J Therm. Ana Calorim.*, 143, 1973–1984 (2021).
- [31] S.A.M. Alsallami, U. Khan, S.U. Khan, A. Ghaffari, M.I. Khan, M.A. Elshorbagy and M.Riaz Khan, Numerical simulations for optimised flow of second-grade nanofluid due to rotating disk with nonlinear thermal radiation: Chebyshev spectral collocation method analysis, *Pramana – J. Phys.*, 96, 98 (2022).
- [32] A.Tassaddiq, S. Khan, M. Bilal, T. Gul, S. Mukhtar, Z. Shah, and E. Bonyah, Heat and mass transfer together with hybrid nanofluid flow over a rotating disk, *AIP Advances*, 10 055317 (2020).
- [33] M. Shoaib, M.A.Z. Raja, M.T. Sabir, K.S. Nisar, W. Jamshed, B.F. Felemban, I.S. Yahia, MHD Hybrid Nanofluid Flow Due to Rotating Disk with Heat Absorption and Thermal Slip Effects: An Application of Intelligent Computing, *Coatings*, 11(12) 1554 (2021).
- [34] H. Waqas, U. Farooq, R. Naseem, S.Hussain and M. Alghamdi, Impact of MHD radiative flow of hybrid nanofluid over a rotating disk, *Case Studies in Thermal Engineering*, 26 101015 (2021).
- [35] M. Ijaz Khan, Transportation of hybrid nanoparticles in forced convective Darcy-Forchheimer flow by a rotating disk, *International Communications in Heat and Mass Transf.*, 122 105177 (2021).
- [36] M. Kumar and P.K. Mondal, Irreversibility analysis of hybrid nanofluid flow over a rotating disk: Effect of thermal radiation and magnetic field, *Colloids and Surfaces A: Physicochemical and Engineering Aspects*, 635 128077 (2022).
- [37] S.M. Mousavi, M. Yousefi, M.N. Rostami, H. Tamim, M. Alimohammadian and S. Dinarvand, Zinc oxide–silver/water hybrid nanofluid flow toward an off-centered rotating disk using temperature-dependent experimental-based thermal conductivity, *Heat Transfer*, 51 4169- 4186 (2022).
- [38] F. Shahzad, W. Jamshed, S.M. El Din, Md. Shamshuddin, R.W. Ibrahim, Z. Raizah, Second-order convergence analysis for Hall effect and electromagnetic force on ternary nanofluid flowing via rotating disk, *Sci Rep.*, 12, 18769 (2022).
- [39] S. Alshahrani, N.A. Ahammad, M. Bilal, M.E. Ghoneim, A. Ali, M.F. Yassen and E. Tag Eldin, Numerical simulation of ternary nanofluid flow with multiple slip and thermal jump conditions, *Front. Energy Res.*, 10 967307 (2022).
- [40] M.D. Shamshuddin, N. Akkurt, A. Saeed and P. Kumam, Radiation mechanism on dissipative ternary hybrid nanofluid flow through rotating disk encountered by Hall currents: HAM solution, *Alexandria Engineering Journal*, 65 543-559 (2023).
- [41] M. Mustafa, MHD nanofluid flow over a rotating disk with partial slip effects: Buongiorno model, *Int. J. Heat Mass Transf.*, 108 1910–1916 (2017).
- [42] N. Acharya, F. Mabood, S.A. Shahzad and I.A. Badruddin, Hydrothermal variations of radiative nanofluid flow by the influence of nanoparticles diameter and nanolayer, *International Communications in Heat and Mass Transfer*, 130 105781 (2022).
- [43] I. Waini, A. Ishak and I.Pop, Multiple solutions of the unsteady hybrid nanofluid flow over a rotating disk with stability analysis, *European Journal of Mechanics - B/Fluids*, 94 121-127 (2022).
- [44] S.A. Khan, T. Hayat and A. Alsaedi, Thermal conductivity performance for ternary hybrid nanomaterial subject to entropy generation, *Energy Reports*, 8 9997-10005 (2022).